Int. J. Heat Mass Transfer. Vol. 41, No. 1, pp. 3–9, 1998

Printed in Great Britain
0017-9310/98 $19.00+0.00

Pergamon

PII: S0017-9310(97)00147-6

A note on the contact temperature during high-Peclet-number flow over a flat substrate

P. S. BASHFORTH
School of Mathematics, University of Bristol, Bristol BS8 1TW, U.K.

J. G. ANDREWS
Nuclear Electric Ltd, Gloucester GL3 7RS, U.K.

and

D. S. RILEY†
Department of Theoretical Mechanics, University of Nottingham, Nottingham NG7 2RD, U.K.

(*Received* 12 *December* 1996 *and in final form* 1 *May* 1997)

Abstract—Knowledge of the temperature at the interface between a hot liquid spreading over a cold solid substrate is important in determining the nature and extent of any freezing of the spreading liquid and/or melting of the substrate. In this paper, a simple model is studied to assess the influence of convection on the spatial and temporal variation of the interface temperature. New solutions are determined by both analytical and approximate numerical techniques. The theoretical and numerical results are compared in the case of slug flow and shown to be in good agreement Shear flow and axisymmetric flow are also considered. © 1997 Elsevier Science Ltd.

1. INTRODUCTION

Heat transfer between two media involving liquid–solid phase transitions is important in both nature and industry. Natural situations include ice formation in rivers, melting of icebergs and lava flows from volcanoes. Industrial areas of interest include casting, welding, hot liquid jets for drilling and the design of heat sinks in power generating systems and in the nuclear power industry. In this last example, the operators are required to demonstrate that adequate safety margins exist even under severe accident conditions. This means that the physical processes involved in extreme conditions are sufficiently understood that corrective actions can be implemented effectively.

The problem motivating the work in this paper is an extreme hypothetical situation in a gas-cooled reactor, where it is supposed that the shutdown systems have failed to arrest some event that has led to the fuel in a particular channel to overheat, causing the entire fuel inventory of that channel to melt and pour onto the steel floor below. This molten fuel material would spread over the floor in a matter of seconds and freeze into a solidified mass. On a much longer time-scale, the solidified fuel would release its nuclear decay heat, partly to the gaseous environment (by radiative heat transfer) and partly to the steel floor (by conduction). The issue of industrial interest is the nature and extent of any floor melting, either during the initial spreading of the molten fuel or later during the release of decay heat.

In considering the possibility of melting of the floor due to the release of decay heat, the extent of spreading of the molten material is a key factor. If the material were to be released rapidly and to spread extensively over the floor, it would form only a thin layer. This would give a weak heat source unable to melt the floor. Similarly if the arrival rate of the molten material were so low that the fluid was broken into droplets as it fell from the fuel channel, these would be dispersed over a wide area by the gas flows, and again the heat source would be weak. The only case of industrial interest is the intermediate regime of moderate flow rates, where the extent of spreading is limited and the heat source may not be insignificant. It is the understanding of this regime that forms the focus of this paper. In particular, we consider the factors controlling the contact temperature at the interface between the spreading puddle and the base. Early melting could lead to the incoming fluid mixing with melted base material, thus enhancing the erosion of the base.

Many studies have been made of a liquid flow over a cold base. One particular problem that has received much attention is the freezing of a warm liquid in steady planar flow over a cold surface, where it is normally assumed that

(1) the thickness of the deposited layer is

†Author to whom correspondence should be addressed.

NOMENCLATURE

- $\hat{a}_1, \hat{b}_1, \hat{c}_1, \hat{a}_2, \hat{b}_2, \hat{c}_2$ coefficients [see equation (26)]
- k thermal conductivity
- $Pe = U^2t/\kappa_1$ Peclet number
- p, q shear and slip values for shear flow
- Q volume flow rate
- r, z cylindrical polar coordinates
- R scaled radial coordinate
- s dimensionless penetration coordinate
- $\hat{s}$ scaled dimensionless penetration coordinate
- S similarity function
- t time
- t' integration variable
- T temperature
- T_0 ambient temperature of the lower medium
- T_∞ ambient temperature of the upper medium
- u velocity component
- U characteristic speed of the leading edge of the spreading fluid
- V dimensionless contact temperature
- x, z Cartesian coordinates.

Greek symbols

- α constant
- $\gamma, \hat{\mu}$ coefficients [see equation (26)]
- κ thermal diffusivity
- $\lambda = (k_2/k_1)\sqrt{(\kappa_1/\kappa_2)}$ dimensionless group
- $\eta = t' + (\lambda^2 - 1)\hat{x}$ compound variable
- θ dimensionless temperature.

Subscripts

- 0 ambient condition in the lower medium
- 1, 2 upper and lower medium quantities, respectively
- fp melting point of UO_2
- mp melting point of steel
- ∞ ambient condition in the upper medium
- $\wedge$ dimensionless quantity.

sufficiently small that heat conduction normal to the substrate dominates (compared with conduction parallel to the interface);

(2) the convective heat flux from the liquid to the solid is a known function of the streamwise coordinate;

(3) the physical properties of the liquid and solid are constant;

(4) the initial temperature of the cold surface is uniform and constant;

(5) there exists a definite interface between the liquid and solid.

Libby and Chen [1] (referred to as LC) found analytical short- and long-time solutions and calculated a complete numerical solution using Goodman's integral method [2]. For short times the classical conduction solution prevails, while at large times a limiting thickness of deposit is approached. Lapadula and Mueller [3] (referred to as LM) developed a simple approximate analytical solution using a variational method. Their numerical results were indistinguishable from LC's, but their differential equation governing the deposit thickness as a function of time had a simpler form than LC's. Beaubouef and Chapman [4] found a numerical solution using finite-differences. Their results for the steady-state convective heat transfer rates showed good agreement with those of LM. Savino and Siegel [5] used an analytical iteration technique to find successive approximations for the deposit thickness and temperature profile. The analytical expressions were of simple form and there was good agreement with the numerical and approximate solutions of LC, LM and, Beaubouef and Chapman. Elmas [6] found a closed-form analytical solution for the deposit thickness, which accommodated time-dependent boundary conditions. Siegel and Savino [7] considered a more general problem where a frozen layer forms from a liquid flow over a flat plate cooled below the freezing temperature of the liquid by a coolant flowing along the other side of the plate. They compared three analytical procedures and presented numerical results graphically, concluding that a method developed in their paper gave a rapidly converging means of solving the problem.

Cheung and Epstein [8] reviewed all this work, pointing out that if the wall is either kept isothermal or convectively cooled below there is a continuous supply of heat sinks at the wall to cool the flow, allowing a constant crust thickness. In many practical situations, including the reactor scenario, the wall is neither cooled in this way nor kept isothermal and, in consequence, conduction within the wall needs to be considered.

Epstein [9] examined this conjugate problem in the case when solidification is the only phase-change occurring. Motivated by applications to lava flows, Huppert [10] analysed the melting and/or freezing that can occur when hot fluid flows turbulently over a cold solid base. The resulting equations were solved using an explicit finite-difference scheme. The main conclusion was that whenever a hot, turbulent flow is confined by a solid surface and the freezing temperature of the fluid exceeds the initial temperature of the solid, the initial response is the formation of a chill (i.e. solidification occurs first). In addition, provided that the turbulent flow is sufficiently deep and that the melting temperature of the solid is less than the temperature of the turbulent flow, the energy flow reverses: there is melting back of the chill and the substrate eventually melts.

In Huppert's problem the molecular conductivities of the fluid and solid base are taken to be equal, but the eddy diffusivity of the turbulently convecting melt is somewhat larger. In the reactor case the solid base has a molecular diffusivity which is an order of magnitude larger than that of the impacting material, but the eddy diffusivity of the material in turbulent flow may be comparable or even dominate. Thus, in practice there will be a range of diffusivity contrasts to consider depending upon the strength of the turbulence. Throughout this work the diffusivity is taken to be greater in the solid (in contrast to Huppert's problem). We consider the early times after a front of fluid passes over part of the base and determine the contact temperature between the fluid and base. By comparing the contact temperature with the fusion temperatures of the materials, we can then determine what phase-changes, if any, are initiated.

The problem considered here bears similarities to the classical Leveque problem for laminar flow heat transfer on a flat plate [11]. The Leveque problem involves a material at some ambient uniform temperature flowing with a linear shear profile over a substrate at a different uniform temperature. There is a self-similar solution for the temperature in the developing thermal boundary layer in terms of an incomplete Gamma function. Yen and Tien [12] assumed the same flow field in determining the temperature distribution in a fluid flowing over a melting plate. They assumed quasi-steady conditions, although account was taken of the movement of the interface due to melting. Using the Leveque solution as the first approximation in an analytical iterative process, they found that the melting resulted in a decrease in the heat transfer coefficient at the surface. Once again the solution was time independent. In the current work it is the initiation of phase-changes that is to be studied and thus the work is time dependent. This means that in general an analytical solution is not possible.

2. TWO-DIMENSIONAL FLOW

To investigate the behaviour of the contact temperature soon after a hot liquid passes over a solid base, a series of model problems is considered. Throughout the work it is assumed that phase-change does not occur, though by analysing the contact temperature an estimate is obtained for phase-changes to be initiated. Two-dimensional flow fields are considered first, and then the axisymmetric case.

2.1. *Specification of the problem*

To fix ideas, consider two semi-infinite media having different thermal properties, one medium initially occupying $x < 0$, $z > 0$ at temperature T_∞, the other $x > 0$, $z < 0$ at temperature T_0. At time $t = 0$, the upper medium starts moving in the positive x-direction with speed u. The geometry is shown in Fig. 1.

The temperature in the upper medium, T_1, satisfies

$$\kappa_1\left(\frac{\partial^2 T_1}{\partial x^2}+\frac{\partial^2 T_1}{\partial z^2}\right)=\frac{\partial T_1}{\partial t}+u\frac{\partial T_1}{\partial x} \qquad (1)$$

while the temperature in the lower medium, T_2, satisfies

$$\kappa_2\left(\frac{\partial^2 T_2}{\partial x^2}+\frac{\partial^2 T_2}{\partial z^2}\right)=\frac{\partial T_2}{\partial t}. \qquad (2)$$

Assuming good thermal contact at the interface between the two materials gives continuity of temperature and heat flux, so that the boundary conditions are

$$T_1 = T_2, \quad k_1\frac{\partial T_1}{\partial z}=k_2\frac{\partial T_2}{\partial z} \quad \text{on } z=0 \qquad (3)$$

where k denotes thermal conductivity, assumed constant. In addition, the incoming fluid is all at its initial temperature, so that

$$T_1 = T_\infty \quad \text{at } x=0. \qquad (4)$$

It is convenient to introduce dimensionless space, time, velocity and temperature variables, $\hat{x}$, $\hat{z}$, $\hat{t}$, $\hat{u}$, and θ by using κ_1/U, κ_1/U^2 and U as length, time and velocity scales and by measuring temperature relative to T_0 in units of $T_\infty - T_0$. Here U is the characteristic speed of the leading edge of the spreading fluid. Assuming that the fluid is moving sufficiently fast, i.e. the Peclet number $Pe = U^2t/\kappa_1$ is large, convection will dominate conduction, except in a thin boundary layer ($\hat{z} = O(Pe^{-1/2})$) where conduction in the $\hat{z}$-direction will balance convection. (Furthermore, if $\hat{x} = O(Pe^{-1/2})$ or $\hat{x}-\hat{u}\hat{t} = O(Pe^{-1/2})$ axial conduction is also important, but consideration of these small regions lies outside the scope of the present analysis). Likewise, provided that $k_1/k_2 = O(1)$ as $Pe \to \infty$,

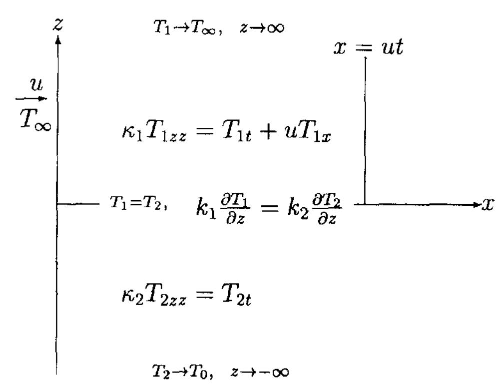

Fig. 1. Schematic representation of the problem.

transverse conduction will dominate longitudinal conduction in the substrate. Thus, in the limit $Pe \to \infty$, the problem reduces to

$$\frac{\partial^2 \theta_1}{\partial \hat{z}^2} = \frac{\partial \theta_1}{\partial \hat{t}} + \hat{u}\frac{\partial \theta_1}{\partial \hat{x}} \quad \hat{x} < \hat{u}\hat{t} \quad \hat{z} > 0 \tag{5}$$

$$\frac{\kappa_2}{\kappa_1}\frac{\partial^2 \theta_2}{\partial \hat{z}^2} = \frac{\partial \theta_2}{\partial \hat{t}} \quad \hat{z} < 0 \tag{6}$$

subject to the boundary conditions

$$\theta_1 \to 1, \hat{z} \to \infty, \theta_2 \to 0, \hat{z} \to -\infty \tag{7}$$

$$\theta_1 = 1, \quad \hat{x} = 0 \tag{8}$$

$$\theta_1 = \theta_2 = V(\hat{x}, \hat{t}), \quad \frac{k_1}{k_2}\frac{\partial \theta_1}{\partial \hat{z}} = \frac{\partial \theta_2}{\partial \hat{z}}, \quad \hat{z} = 0 \tag{9}$$

where $V(\hat{x}, \hat{t})$ is the unknown dimensionless contact temperature.

2.2. *Slug flow*

The simplest velocity distribution featuring a moving front is when u is uniform, $u = U$, say (so that $\hat{u} = 1$). This introduces the necessary convection without over-complicating the problem. In particular, analytical solutions for the temperature profiles in both materials exist in this case.

To find the solution, a double Laplace transform with respect to $\hat{t}$ and $\hat{x}$ is taken. The region $0 < \hat{x} < \infty$ over which the transform is taken actually extends beyond the physical extent of the fluid. However, the point of view is adopted that the method is applied purely formally and the solution is verified *a posteriori*. Jaeger [13] was one of the first to demonstrate the utility of such an approach in his work on unsteady conduction in two-dimensions. Omitting the straightforward detail, the solution satisfying the equations and boundary conditions of the original problem is

$$\theta_1(\hat{x}, \hat{z}, \hat{t}) = \operatorname{erf}\left[\frac{\hat{z}}{2\sqrt{\hat{x}}}\right] + \frac{2}{\pi}\exp\left[\frac{-\hat{z}^2}{4\hat{x}}\right]\arctan\left[\frac{1}{\lambda}\sqrt{\left(\frac{\hat{t}}{\hat{x}} - 1\right)}\right] - \frac{\lambda \hat{z}}{2\sqrt{\pi}}\int_{\hat{x}}^{\hat{t}} \exp\left[\frac{-\hat{z}^2\lambda^2}{4\eta}\right] \times \operatorname{erfc}\left[\frac{\hat{z}}{2}\sqrt{\left(\frac{t' - \hat{x}}{\hat{x}\eta}\right)}\right]\frac{dt'}{\eta^{3/2}} \tag{10}$$

$$\theta_2(\hat{x}, \hat{z}, \hat{t}) = \frac{\lambda}{\pi}\sqrt{\hat{x}}\int_{\hat{x}}^{\hat{t}} \operatorname{erfc}\left[\frac{-\hat{z}\sqrt{\kappa_1}}{2\sqrt{\kappa_2(\hat{t} - t')}}\right]\frac{dt'}{\eta\sqrt{t' - \hat{x}}}, \quad \hat{x} < \hat{t} \tag{11}$$

where $\eta = t' + (\lambda^2 - 1)\hat{x}$ and $\lambda = k_1/k_2\sqrt{\kappa_2/\kappa_1}$.

The contact temperature, which is given by

$$V(\hat{x}, \hat{t}) = \frac{2}{\pi}\arctan\left\{\frac{1}{\lambda}\left(\frac{\hat{t}}{\hat{x}} - 1\right)^{1/2}\right\}, \hat{x} < \hat{t} \tag{12}$$

is constant on a trajectory $\hat{x} = \alpha\hat{t}$, where α is a constant $(0 \leqslant \alpha \leqslant 1)$. In particular, the contact temperature is unity on $\hat{x} = 0$ (i.e. $\alpha = 0$) and is zero on $\hat{x} = \hat{t}$ (i.e. $\alpha = 1$). So if the dimensionless freezing temperature of the fluid is between 0 and 1 solidification will occur and similarly, if the dimensionless melting point of the base lies in this range, melting of the base will occur.

Figure 2 shows the dimensionless contact temperature against $\hat{x}/\hat{t}$ for a range of values of λ. It can be seen that the contact temperature decreases as the distance from $\hat{x} = 0$ increases. The fluid near $\hat{x} = 0$, which has only recently come into contact with the cold base, has been subject to only a small amount of cooling, resulting in little temperature change. In contrast, the fluid near the spreading front has been under the cooling influence of the base for some time and thus has been cooled substantially. This effect is most pronounced for the larger values of λ since the conductivity of the base relative to that of the fluid is high in this case.

This problem can be solved approximately using Goodman's integral method, an approach that more readily accommodates general velocity profiles than the transform technique. We define dimensionless penetration coordinates s_1 and s_2 in the upper and lower materials, respectively, such that for $\hat{z} > s_1$ and $\hat{z} < s_2$ the materials are at their respective ambient temperatures. The heat balance equations result from integrating equations (5) and (6) from $\hat{z} = 0$ to s_1 and s_2, respectively. Assuming quadratic temperature profiles

$$\theta_1(\hat{x}, \hat{z}, \hat{t}) = 1 - (1 - V)\left(1 - \frac{\hat{z}}{s_1}\right)^2,$$

$$\theta_2(\hat{x}, \hat{z}, \hat{t}) = V\left(1 - \frac{\hat{z}}{s_2}\right)^2 \tag{13}$$

the heat balance integrals in each region and the heat flux condition at the interface give three equations for the three unknowns $s_1(\hat{x}, \hat{t})$, $s_2(\hat{x}, \hat{t})$ and $V(\hat{x}, \hat{t})$,

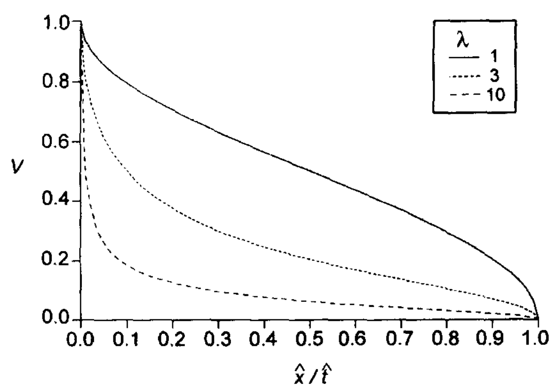

Fig. 2. Contact temperature vs $\hat{x}/\hat{t}$, in the cases $\lambda = 1$, 3 and 10.

$$k_1 s_2(1-V)+k_2 s_1 V = 0, \quad s_2\frac{\partial}{\partial \hat{t}}(V s_2) = 6\frac{\kappa_2}{\kappa_1}V$$

$$s_1\left(\frac{\partial}{\partial \hat{t}}+\hat{u}\frac{\partial}{\partial \hat{x}}\right)[s_1(1-V)] = 6(1-V). \qquad (14)$$

Rescaling s_1 and s_2 so that

$$\hat{s}_2 = \frac{k_1}{k_2}s_2 \quad \text{and} \quad \hat{s}_1 = s_1 \qquad (15)$$

and eliminating $V(\hat{x},\hat{t})$ gives

$$6(\hat{s}_2-\hat{s}_1) = \hat{s}_1(2\hat{s}_2-\hat{s}_1)\left(\frac{\partial}{\partial \hat{t}}+\frac{\partial}{\partial \hat{x}}\right)\hat{s}_1 - \hat{s}_1^2\left(\frac{\partial}{\partial \hat{t}}+\frac{\partial}{\partial \hat{x}}\right)\hat{s}_2 \qquad (16)$$

$$\frac{6}{\lambda^2}(\hat{s}_2-\hat{s}_1) = \hat{s}_2^2\frac{\partial \hat{s}_1}{\partial \hat{t}}+\hat{s}_2(\hat{s}_2-2\hat{s}_1)\frac{\partial \hat{s}_2}{\partial \hat{t}} \qquad (17)$$

subject to

$$\hat{s}_1(0,\hat{t}) = \hat{s}_2(\hat{t},\hat{t}) = \hat{s}_2(\hat{x},0) = 0.$$

The simplest way of solving the above equations is to utilize the fact that they admit a similarity solution, namely

$$\hat{s}_1 = \sqrt{\hat{t}}S_1(\hat{x}/\hat{t}), \quad \hat{s}_2 = \sqrt{\hat{t}}S_2(\hat{x}/\hat{t}). \qquad (18)$$

Of wider application, however, is the method of characteristics and it is this we choose to employ. The following differential relationships hold along characteristics,

$$0 = \hat{s}_1(2\hat{s}_2-\hat{s}_1)\,\mathrm{d}\hat{s}_1 - \hat{s}_1^2\,\mathrm{d}\hat{s}_2 - 6(\hat{s}_2-\hat{s}_1)\,\mathrm{d}\hat{t} \quad \text{along}\ \frac{\mathrm{d}\hat{x}}{\mathrm{d}\hat{t}} = 1 \qquad (19)$$

$$0 = \hat{s}_2^2\,\mathrm{d}\hat{s}_1 + \hat{s}_2(\hat{s}_2-2\hat{s}_1)\,\mathrm{d}\hat{s}_2 - \frac{6}{\lambda^2}(\hat{s}_2-\hat{s}_1)\,\mathrm{d}\hat{t} \quad \text{along}\ \frac{\mathrm{d}\hat{x}}{\mathrm{d}\hat{t}} = 0. \qquad (20)$$

Approximating by first-order finite differences gives a simple numerical scheme for finding the solution. The initial conditions are $\hat{s}_1 = \hat{s}_2 = 0$ and the boundary conditions are $\hat{s}_1 = 0$ on $\hat{x} = 0$ and $\hat{s}_2 = 0$ on $\hat{x} = \hat{t}$. There are singularities at time $\hat{t} = 0$ and at $\hat{x} = 0$, $\hat{x} = \hat{t}$, so these conditions cannot be used directly in the numerical scheme. However, it is straightforward to show from using (18) in (16) and (17) that

$$\hat{s}_1 \sim \sqrt{12\hat{x}}, \quad \hat{s}_2 \sim -\frac{1}{\lambda}\sqrt{6(\hat{t}-\hat{x})}, \quad \hat{x}\sim\hat{t} \qquad (21)$$

$$\hat{s}_1 \sim \sqrt{6\hat{x}}, \quad \hat{s}_2 \sim -\frac{1}{\lambda}\sqrt{12\hat{t}}, \quad 0<\hat{x}\ll\hat{t} \qquad (22)$$

which can be used to avoid the singularities.

Once $\hat{s}_1$ and $\hat{s}_2$ are known at each time step, the dimensionless contact temperature, V, follows from rearranging the first equation of (14),

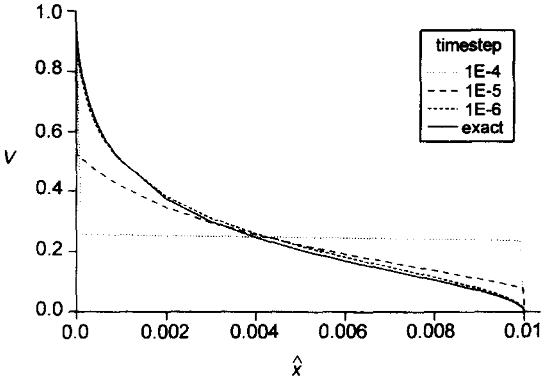

Fig. 3. Contact temperature for a range of time steps, in the case $\lambda = 3$.

$$V = \frac{k_1 s_2}{k_1 s_2 - k_2 s_1} = \frac{\hat{s}_2}{\hat{s}_2-\hat{s}_1}. \qquad (23)$$

Figure 3 shows the dimensionless contact temperature from (12) together with the results from the finite-difference scheme for a range of time steps. The approximate numerical solution agrees well with the exact answer, provided a sufficiently small time step is used. In the results presented, the solutions were initiated at 10^{-8}, using (21), and the smallest time step used was 10^{-6}.

2.3. *Shear flow*

Taking a linear shear velocity profile $u = pz+q$ where $q \neq 0$ and p are constants, gives a more realistic flow over a solid surface. Since the key interest is in the contact temperature, it is the flow in the vicinity of the interface that is most important. The linear shear velocity gives a flow field that models a boundary-layer velocity distribution near this interface.

The use of the transform technique becomes technically complex in this case and so only the heat balance method is employed. We use the same technique and temperature profiles as before, but with $U = q$, and obtain

$$0 = \hat{a}_1\frac{\partial \hat{s}_1}{\partial \hat{t}} + \hat{b}_1\frac{\partial \hat{s}_2}{\partial \hat{t}} + \hat{c}_1 \qquad (24)$$

$$0 = \hat{a}_2\left(\frac{\partial}{\partial \hat{t}}+\hat{\mu}\frac{\partial}{\partial \hat{x}}\right)\hat{s}_1 + \hat{b}_2\left(\frac{\partial}{\partial \hat{t}}+\hat{\mu}\frac{\partial}{\partial \hat{x}}\right)\hat{s}_2 + \hat{c}_2 \qquad (25)$$

where

$$\hat{a}_1 = \hat{s}_2^2,$$

$$\hat{a}_2 = \hat{s}_1\hat{s}_2[4(2\hat{s}_2-\hat{s}_1)+\gamma\hat{s}_1(3\hat{s}_2-2\hat{s}_1)]$$

$$\hat{b}_1 = \hat{s}_2(\hat{s}_2-2\hat{s}_1),$$

$$\hat{b}_2 = -\hat{s}_1^2\hat{s}_2(4+\gamma\hat{s}_1)$$

$$\hat{c}_1 = -\frac{6}{\lambda^2}(\hat{s}_2-\hat{s}_1),$$

$$\hat{c}_2 = -\frac{3\gamma}{\lambda^2}\hat{s}_1^3 - 3\hat{s}_2[8(\hat{s}_2-\hat{s}_1)+\gamma\hat{s}_1(3\hat{s}_2-4\hat{s}_1)]$$

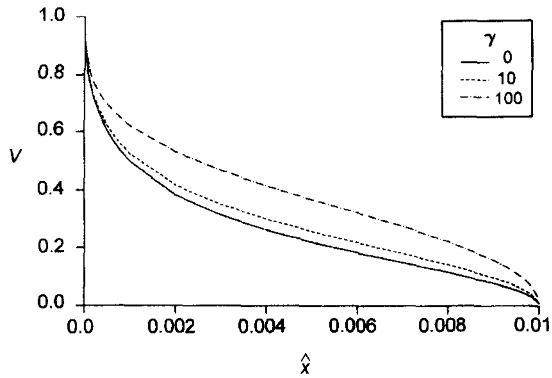

Fig. 4. Contact temperature for a range of values γ with $\lambda = 3$, at $\hat{t} = 0.01$.

$$\gamma = \frac{p\kappa_1}{q^2},$$

$$\hat{\mu} = \frac{8(\hat{s}_2 - \hat{s}_1) + \gamma\hat{s}_1(3\hat{s}_2 - 2\hat{s}_1)}{8(\hat{s}_2 - \hat{s}_1)}. \quad (26)$$

The differential relationships for $\hat{s}_1$ and $\hat{s}_2$ along the characteristics are

$$0 = \hat{a}_1\,\mathrm{d}\hat{s}_1 + \hat{b}_1\mathrm{d}\hat{s}_2 + \hat{c}_1\,\mathrm{d}\hat{t} \quad \text{along}\,\frac{\mathrm{d}\hat{x}}{\mathrm{d}\hat{t}} = 0 \quad (27)$$

$$0 = \hat{a}_2\,\mathrm{d}\hat{s}_1 + \hat{b}_2\,\mathrm{d}\hat{s}_2 + \hat{c}_2\,\mathrm{d}\hat{t} \quad \text{along}\,\frac{\mathrm{d}\hat{x}}{\mathrm{d}\hat{t}} = \hat{\mu}. \quad (28)$$

These are solved in a similar way to the uniform-velocity problem. In this case, however, the second set of characteristics have to be determined with the solution (since they are no longer lines of constant slope).

Figure 4 shows the dimensionless contact temperature for a range of values of the parameter γ. For fixed q and κ_1, this is equivalent to a range of values of p and thus the figure shows the effect of the shear velocity on the results. As the shear increases (γ increasing), the flow increases, and thus the contact temperature increases. $\gamma = 0$ corresponds the no-shear case, solved in the previous section. It can be seen that there is little effect on the contact temperature until γ reaches about 10 in the example with $\lambda = 3$. In general the effect of the shear is most marked in the middle, away from the end effects of the leading front and the point of initiation of the flow.

3. AXISYMMETRIC FLOW

In many situations, including the reactor scenario, the flow will not be two-dimensional, but may be spreading out from a source axisymmetrically. With a constant volume flow rate per unit length of Q m^2 s^{-1}, there is a radial velocity u_r, of $Q/2\pi r$, and, in the large-Peclet-number limit, the dimensionless temperature in the upper medium satisfies

$$\frac{\partial^2\theta_1}{\partial\hat{z}^2} = \frac{\partial\theta_1}{\partial\hat{t}} + \frac{Q}{2\pi\kappa_1\hat{r}}\frac{\partial\theta_1}{\partial\hat{r}} \quad (29)$$

whilst that in the lower medium satisfies equation (6), as before. Here $\hat{r}$ and $\hat{z}$ denote dimensional cylindrical polar coordinates and variables have been non-dimensionalised as before. Introducing $R = \pi\kappa_1\hat{r}^2/Q$, transforms the equations to

$$\hat{z} > 0: \frac{\partial^2\theta_1}{\partial\hat{z}^2} = \frac{\partial\theta_1}{\partial\hat{t}} + \frac{\partial\theta_1}{\partial R} \quad (30)$$

$$\hat{z} < 0: \frac{\kappa_2}{\kappa_1}\frac{\partial^2\theta_2}{\partial\hat{z}^2} = \frac{\partial\theta_2}{\partial\hat{t}}. \quad (31)$$

which have the same form as the two-dimensional case, the boundary conditions being unchanged. In particular the dimensionless contact temperature is

$$V(\hat{r},\hat{t}) = \frac{2}{\pi}\arctan\left\{\frac{1}{\lambda}\left(\frac{Q\hat{t}}{\pi\kappa_1\hat{r}^2} - 1\right)^{1/2}\right\}, \hat{r} < \sqrt{\frac{Q\hat{t}}{\pi\kappa_1}}. \quad (32)$$

Thus the results for the axisymmetric flows can be obtained from those of the two-dimensional solutions by a simple transformation. This means that the results are qualitatively the same as those given in Section 2.2 (and Section 2.3). In particular the effects of the parameters λ (and γ) will be the same.

4. DISCUSSION OF THE RESULTS

The parameter λ has the approximate value 3 for the case of UO_2 on steel. Typically the steel base is initially about 500 K and the UO_2 has little superheat with a temperature of around 3200 K. In this case $\theta = (T - 500)/2700$. Thus the melting points of UO_2 and steel correspond to $\theta_{fp} = 0.97$ and $\theta_{mp} = 0.48$, respectively.

For the constant velocity case, Fig. 2 suggests that there would be initiation of a crust of UO_2 along all the interface, apart from a very small portion near $x = 0$. In addition the initiation of melting of the steel is predicted from $x = 0$ along about 1/10th of the distance covered by the flow. Thus if the flow front had travelled 0.5 m, this predicts melting of the steel to about 5 cm from the source with a UO_2 crust over all, but a few millimetres. From Fig. 4, increasing the shear of the flow would have little effect upon the formation of the UO_2 crust, but would increase the distance along which melting of the base occurs. For $\gamma = 100$ the length over which melting occurs is approximately double that for no shear.

Increasing the superheat of the UO_2, so that the initial temperature is say 4000 K, gives $\theta = (T - 500)/3500$, $\theta_{fp} = 0.75$ and $\theta_{mp} = 0.37$. This slightly increases the area near $x = 0$ without crust formation, and approximately doubles the area where melting occurs. However, it is likely that the UO_2 would have other substances from the reactor core mixed in it (for example graphite or steel cladding), and the resulting eutectic would have a lower melting point, of about 2500 K. In this case with 80 K of superheat, $\theta = (T-500)/2080$, $\theta_{fp} = 0.96$ and $\theta_{mp} = 0.63$. The area of crust formation is little changed, whilst the area over which melting occurs is reduced by over half. From Fig. 4, the latter effect is more marked for larger shear velocities (higher γ).

In general the results indicate that a crust forms in the UO_2 fluid over all except a small area of the interface and that melting of the steel base occurs over a larger area. The size of this latter area depends upon the melting temperature and the initial superheat of the fluid flow, while the area of crust formation is relatively unaffected by these parameters.

Many previous models of the early development in contact problems have simplistically assumed two stationary media. The work of this paper shows that the motion of the fluid can significantly effect the detailed spatial and temporal variation of the contact temperature, with the consequent implications on the possible breakthrough of the solid substrate. However, the particular model for the fluid flow assumed in this paper (slug or shear flow) is also simplistic, and more realistic regimes need to be studied. Moreover, local analysis would need to be carried out for $\hat{x} = O(Pe^{-1/2})$ and $\hat{x}-\hat{u}\hat{t} = O(Pe^{-1/2})$ where axial temperature gradients are as important as transverse gradients.

In the past, further progress has been achieved by restricting attention to the effects of phase change on developed flows. The current work has considered a complementary problem involving a developing flow field whilst ignoring phase-change effects. The next step is to incorporate phase changes into the developing flow problem, i.e. the formation of a freezing layer adjacent to the substrate and/or melting of the substrate itself. These effects add considerably to the complexity of the problem, requiring consideration of perturbations to the velocity field and of mixing processes. Such issues will be addressed in future work.

Acknowledgements—PSB acknowledges the support of EPSRC and Nuclear Electric plc through a CASE award.

REFERENCES

1. Libby, P. A. and Chen, S., The growth of a deposited layer on a cold surface. *International Journal of Heat and Mass Transfer*, 1965, **8**, 395–402.
2. Goodman, T. R., Heat-balance integral and its application to problems involving a change of phase. *ASME Transactions C*, 1958, **80**, 335–342.
3. Lapadula, C. and Mueller, W. K., Heat conduction with solidification and a convective boundary condition at the freezing front. *International Journal of Heat and Mass Transfer*, 1966, **9**, 702–704.
4. Beaubouef, R. T. and Chapman, A. J., Freezing of fluids in forced flow. *International Journal of Heat and Mass Transfer*, 1967, **10**, 1581–1587.
5. Savino, J. M. and Siegel, R., An analytical solution for the solidification of a moving warm liquid onto an isothermal cold wall. *International Journal of Heat and Mass Transfer*, 1969, **12**, 803–809.
6. Elmas, E., On the solidification of a warm liquid flowing over a cold wall. *International Journal of Heat and Mass Transfer*, 1970, **13**, 1060–1062.
7. Siegel, R. and Savino, J. M., An analysis of the transient solidification of a flowing warm liquid on a convectively cooled wall. *Third International Heat Transfer Conference Proceedings*, Vol. 4, 1966, pp. 141–151.
8. Cheung, F. B. and Epstein, M., Solidification and melting in fluid flow. In *Advances in Transport Processes*, A.S. Majumdar and R. A. Mashelkar. Wiley, New York, 1984, pp. 35–117.
9. Epstein, M., The growth and decay of a frozen layer in forced flow. *International Journal of Heat and Mass Transfer*, 1976, **19**, 1281–1288.
10. Huppert, H. E., Phase changes following the initiation of a hot turbulent flow over a cold solid surface. *Journal of Fluid Mechanics*, 1989, **198**, 293–319.
11. Knudsen, J. G. and Katz, D. L., *Fluid Dynamics and Heat Transfer*. McGraw-Hill, New York, 1958.
12. Yen, Y. C. and Tien, C., Laminar heat transfer over a melting plate, the modified Leveque problem. *Journal of Geophysics Research*, 1963, **68**, 3673–3678.
13. Jaeger, J. C., The solution of boundary value problems by a double Laplace transformation. *Bulletin of the American Mathematical Society*, 1940, **46**, 687–693.